MONITORING AND ANALYSING PRESSURES AROUND A TBM

A. Bezuijen
Ghent University, Ghent, Belgium and Deltares, Delft, the Netherlands

S. P. Steeneken
Delft University of Technology, Delft, the Netherlands

J. A. T. Ruigrok
Adviesbureau NoordZuidlijn/Witteveen+Bos, Amsterdam, the Netherlands

ABSTRACT: The excess pore pressure in front of a TBM is described for a slurry shield as well as an earth pressure balance (EPB) shield when drilling in saturated sand. Excess pore water pressures are described by using Darcy's law and theory to describe slurry behaviour. Measured pore pressures close to the TBM are explained for various phases of the tunnelling process.

Grout pressures were measured and the possibility how these can cause deformation of the tail shield is discussed. The results of this research has led to a better understanding of the mechanisms and were also used in practice in the design and execution of tunnel projects.

1. INTRODUCTION

Dutch experience of using TBM tunnelling is relatively recent. The first TBM tunnel was constructed in the Netherlands between 1997 and 1999 (the Second Heinenoord Tunnel). In the early 1990s, Dutch engineers were uncertain whether the soft saturated soil in the western parts of their country was suitable for TBM tunnelling. The decision was therefore taken to include a measurement programme in the first tunnelling projects. An overview of this programme and some results are presented by Bakker & Bezuijen (2008). In the programme, results from the measurements were predicted using existing calculation models. The measurement results were analysed at a later date, and discrepancies with the predictions were explained where possible.

An important part of the measurements and analyses in the programme was dictated by the processes that occur around the TBM. An overview of the processes around the TBM studied is described by Bezuijen & Talmon (2009). This paper deals with some of these processes in more detail, because after 2009 some new theory is developed, or existing theory was used to solve problems in field applications. Two aspects will be focused on: the excess pore water pressure at the tunnel face when drilling in saturated sand and the pressure distribution around a TBM shield, due to grouting pressures.

2. EXCESS PORE PRESSURES IN FRONT OF A TBM

2.1. DURING DRILLING

The usual tunnelling conditions in The Netherlands and other deltaic areas are a saturated sandy soil, often medium-fine sand. In such soil conditions, the groundwater flow influences the plastering. There can be a limited plastering of the tunnel face by the bentonite or the muck during drilling of a slurry shield, because the groundwater in front of the TBM prevents water in the bentonite slurry or muck flowing into the soil. Full plastering will only occur during standstill of the TBM process.

Figure 1 shows measured pore pressure in front of a slurry shield as a function of the distance from the TBM front. Plastering occurs during standstill, resulting in a pressure of 120 kPa (the hydrostatic pressure) in the soil. Higher pore pressures were measured during drilling, because the TBM's cutter head removes a cake before it can fully form at the tunnel face. Figure 2 shows the same phenomenon measured in front of an EPB shield. Here, only the maximum pressure during drilling was recorded.

Figure 1 and Figure 2 also show a theoretical curve (Bezuijen, 2002):

$$\phi = \phi_0 (\sqrt{1 + (x/R)^2} - x/R) \qquad (1)$$

Where ϕ_0 is the piezometric head at the tunnel face in front of the infiltrated zone, ϕ the piezometric head at a distance x in front of the tunnel face, and R the radius of the tunnel, assuming a piezometric head of zero far from the tunnel in the pore water, see Figure 3.

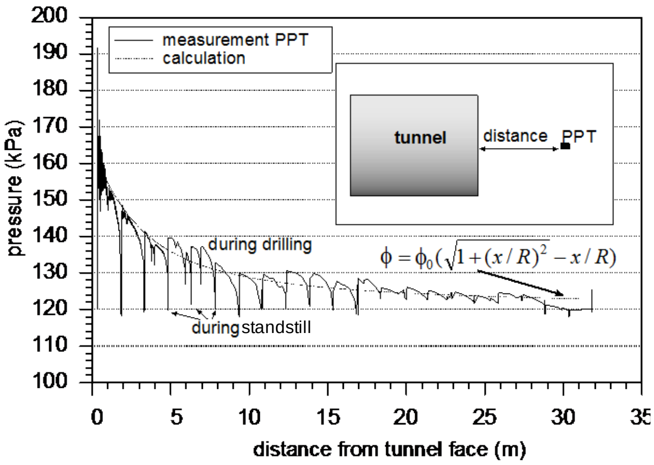

Figure 1: Measured excess pore pressure in front of a slurry shield and approximation.

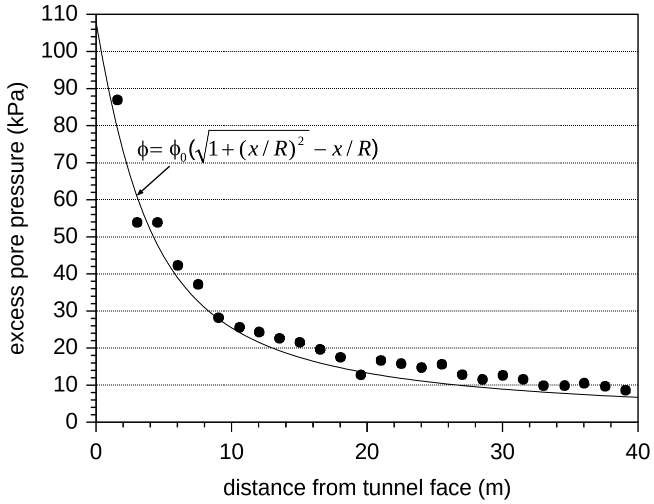

Figure 2: Measured excess pore pressure in front of an EPB shield (•) and approximation (Botlek Rail Tunnel, MQ1 South). Relatively impermeable subsoil.

This relationship is valid for situations where the permeability of soil around the tunnel is constant. This theory was developed already some time ago (Bezuijen et al. 2001, Bezuijen 2002). It was used during the construction of the Green Hart Tunnel in The Netherlands (Aime et al, 2004). The groundwater flow in front of the TBM was in that case not calculated with Equation (1), which is only valid for homogeneous soil conditions, but 3-D finite element calculations were used.

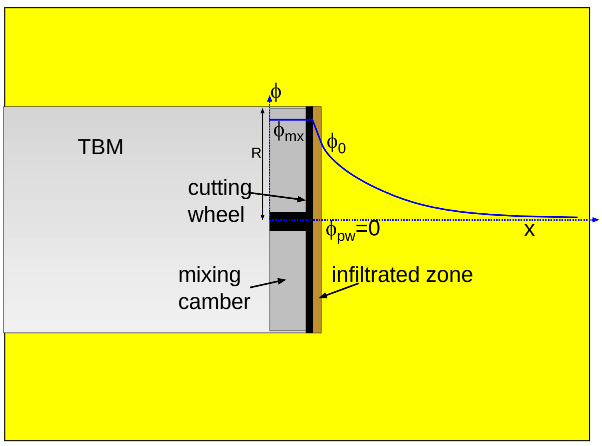

Figure 3: Definition sketch. TBM, infiltration zone and piezometric head.

During the construction of the N/S line in Amsterdam it appeared that the crossing of one of the bridges was rather critical (Kaalberg et al. 2014). The stability of the tunnel face was calculated using 3-D numerical calculations taking into account the influences of excess pore water pressures in front of the tunnel face. The pore pressure distribution in these calculations was calculated with Equation (1). In this project it appears that ϕ_0 was not equal to the pressure in the mixing chamber but has a lower value. A value of α was introduced, defined as:

$$\phi_0 = \alpha(\phi_{mx} - \phi_{pw}) \qquad (2)$$

Where ϕ_{mx} is the piezometric head in the mixing chamber and ϕ_{pw} the piezometric head far from the tunnel in the soil. By measuring the piezometric head close to the TBM during drilling, it was determined that α was 0.6.

The value of α depends on the penetration velocity of the slurry for a slurry shield or the muck for an EPB shield. If the penetration velocity of the slurry is lower than the drilling velocity there will be no effective plastering and α will be close to 1. If on the other hand the penetration velocity of the slurry or muck is larger than the drilling velocity, then α will be smaller than 1. Differentiation of Equation (1) to x results in the hydraulic gradient for x=0, thus at the tunnel face:

$$i = \frac{\phi_0}{R} \qquad (3)$$

With Darcy's law and the relation between filter velocity and pore velocity (v_p), this leads to:

$$v_p = \frac{k\phi_0}{nR} \qquad (4)$$

When α =1, this relation can be used to calculate the penetration rate of the slurry or muck, which will be equal to the pore velocity. If for α=1 the calculated penetration velocity of the slurry or muck is larger than the drilling velocity of the TBM, the slurry or muck will penetrate further into the soil in front of the TBM. Due to the higher viscosity of the slurry than the viscosity of water and the yield stress of the slurry or muck, the penetration rate will slow down and after some penetration, the penetration rate will be equal to the drilling velocity. Now Equation (4) in combination with Equation (2) can be used again, but with a porewater velocity v_p that is equal to v_{TBM}, the drilling velocity, because after the initial faster penetration, the slurry or muck penetration in the soil will have the same velocity as the drilling velocity of the TBM. This allows to calculate α (Steeneken, 2016):

$$\alpha = \frac{nRv_{TBM}}{(\phi_{mx} - \phi_{pw})k} \qquad (5)$$

This result makes it possible to estimate whether excess pore water pressures can be expected in front of a tunnel face when drilling in homogeneous saturated sandy soil. When α calculated with Equation (5) is larger than 1 then v_{TBM} is larger than v_p and the equality $v_p = v_{TBM}$ is not valid anymore. In that case v_p has to be determined by Equation (4) with $\phi_0=\phi_{mx}-\phi_{pw}$ leading automatically to α=1.

Note that no parameters of the slurry are included in the equations above. Implicitly it is assumed that there is a finite slurry penetration which is larger than the scraping depth of the tooth on the cutter wheel (typically 1 or a few centimetres). It is further assumed that the penetration depth is small compared to the radius of the TBM. Anagnostou & Kovari (1994) describe a calculation model for large penetration depths.

2.2. BEFORE AND AFTER DRILLING

After drilling

During standstill, for example because of ring building, the penetration of slurry or muck in the soil will continue until the maximum penetration depth is reached. Assuming that the slurry or muck behaves as a Bingham liquid and that at the maximum penetration depth the pressure drop over the penetrated slurry is taken by the yield stress in the slurry or muck, so that there is no flow, and further assuming that there is a linear relation between the penetration depth and the percentage of the pressure difference that is taken by the yield stress it is possible to model this penetration. Such a model is made by Bezuijen et al. (2001). However, the parameters in that model are not generally known. Therefore the equations has been rewritten such that the necessary parameters can be obtained from a slurry or muck penetration test (Talmon et al. 2013) or can be estimated from pore pressure measurements close to the tunnel, see below.

Assume the situation that there is hardly any slurry or muck penetration during drilling. When drilling stops, the slurry starts to penetrate into the soil. The maximum penetration depth is L. Assume again a piezometric head that is zero far from the tunnel. In that case Equation (4) presents the relation between the piezometric head in the soil just in front of the slurry and the piezometric head in the mixing chamber can be written as:

$$\phi_{mx} = \phi_0 + \frac{nv_p}{k_g} x + \frac{\phi_{mx}}{L} x \qquad (6)$$

Where k_g is the permeability of the soil for the slurry or muck. Since $v_p = dx/dt$ this leads to the equation:

$$\frac{dx}{dt} = \frac{\phi_{mx}(1 - x/L)}{\left(\frac{n}{k} R + \frac{n}{k_g} x\right)} \qquad (7)$$

Equation (7) is a non-linear differential equation. This can be solved numerically starting at x=0 if there is no slurry penetration during drilling and starting with a certain value of x if there had been slurry or muck penetration during drilling. When $dx/dt = v_p$ is determined, Equation (4) can be used to determine ϕ_0 as a function of time. This procedure is used to simulate the measured pressure drop at the end of drilling of one of the rings of the North/South line, using the parameters mentioned in Table 1. As mentioned before, it was measured that for these rings $\alpha = 0.6$ that means that there is always some slurry that is penetrated into the soil in front of the TBM also during drilling. Thus the integration should not start with x=0 m, but with the value of x that corresponds with a piezometric head that is 0.6 times the piezometric head in the mixing camber. This appeared to be x=0.0534 m. Figure 4 shows the result for α=1 and α=0.6. The difference is small. Both lines showed good agreement with the measured values.

Table 1. Parmeters used in calculations for N/S line and GHT. The values of *L* are extrapolated from laboratory tests (Steeneken, 2016).

Parameter	*N/S line*	*GHT*	
k_g	*5.00E-06*	*2.00E-05*	*m/s*
k	*1.00E-04*	*4.00E-04*	*m/s*
L	*0.25*	*0.007*	*m*
ϕ_{mx}	*14.3*	*4.16*	*m*
N	*0.35*	*0.35*	*-*
R	*3.44*	*0.725*	*m*

Krause (1987) suggested an empirical formula for the penetration of the slurry into the soil, determined with experimental data from column infiltration tests:

$$x(t) = \frac{t}{a + t} L \qquad (8)$$

Where a is the timespan to reach half of the final infiltration depth (*0.5L*). This parameter has to be determined by slurry infiltration tests. This parameter depends on the flow regime in an infiltration test. Differentiation of Equation (8) results in:

$$\frac{dx}{dt} = \frac{a}{(a + t)^2} L \qquad (9)$$

For t=0 and x=0 this can be compared with Equation (7) leading to:

$$a = \frac{nRL}{\phi_{mx} k} \qquad (10)$$

The parameter a as defined by Krause will thus depend for example on radius of the tunnel. The procedure followed to derive Equation (10) is a bit 'tricky', because integration of Equation (7) will lead to another equation than the empirical Equation (8). It is therefore possible that also dx/dt at t=0 is different. To check this x in function of t was determined using numerical integration of Equation (7). With non-linear regression this curve was fitted to Equation (8), see Figure 5. There appears to be only a reasonable agreement. At larger values of t, the infiltration is underestimated by Equation (8). The a that follows from the non-linear regression, 149 s, is also in reasonable agreement with a calculated from Equation (10), 211 s. A better agreement is possible by assuming that the L as defined by Krause can be different from the L used in the numerical calculation. Thus in the non-linear regression analysis L in Equation (8) is replaced by $c.L$ where c can vary, but should be approximately 1. This allows a much better agreement, see also Figure 5 and the resulting a from non-linear regression is now 247s also in better agreement with the 211s calculated with Equation (10). Therefore Equation (10) can be used to have a first estimation of a for the situation in front of a TBM drilling in saturated sand if L is determined as a function of ϕ_{mx}, in an infiltration test. The value of a can be of importance in tunnelling because it determines the time span until the cake in front of the TBM is fully formed. This is important when air pressure has to be applied at the tunnel face.

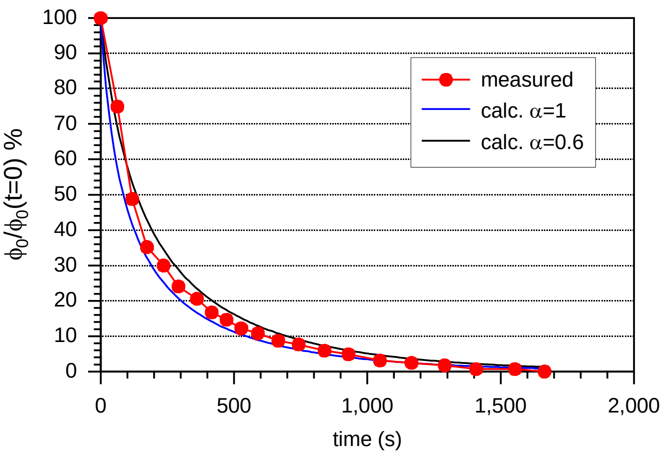

Figure 4: Decrease of excess pore pressure when drilling stops due to slurry penetration. Calculations compared with measurements.

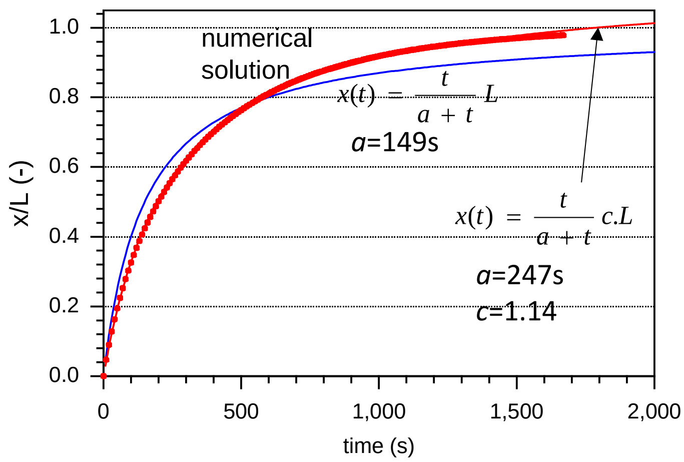

Figure 5: Numerical solution (dots) compared with curve proposed by Krause (1987), see also text.

Start of drilling

The principle described above can also be used to estimate the increase in excess pore water pressure when drilling starts. Again Equation (7) can be used, but it should be realized that during drilling the cutting wheel takes some soil in which the slurry or muck is penetrated. And therefore to calculate x at various time steps the reduction x due to drilling has to be added:

$$x_{i+1} = x_i + \left(\frac{dx}{dt} - v_{TBM}\right)\Delta t \qquad (8)$$

Where the suffixes i and $i+1$ refer to different times in a numerical solution and Δt is the time step between them. Comparing the results of such a calculation with the measured pressure increase for the GHT (parameters see Table 1) with a slurry shield showed only a reasonable agreement. A possible cause is that the model of the slurry as a Bingham liquid that penetrates into the soil may be too simple. Talmon et al. (2013) have shown that slurry penetration into the soil is composed of two different processes. A mudspurt, which agrees well with the model described in this paper and the formation of an external filter cake. The external filter cake is not taken into account in this model. When drilling starts the external filter cake will be removed immediately; and this may result in an faster pressure rise than according to this model. Furthermore, it is unlikely that there is a sharp boundary in the soil between the soil where the slurry has penetrated and the soil without slurry.

Although the model has therefore some limitations, it presents an interesting possibility to make an estimate of the distance the slurry has penetrated into the soil for the situation that the pore pressures are measured but there is no information on the penetration depth. In the first calculation steps using Equation (8), dx/dt will be close to zero and thus x will shorten each time step with $v_{TBM}.\Delta t$. This allows for a graphical solution to determine L, see Figure 7. To test this procedure, the data for the GHT simulation were used and a penetration depth of 0.088 m is found, while 0.07 m was used as input data.

It has to be tested on more data to determine how accurate this procedure is, but it seems promising. It is also possible to estimate the infiltration depth using the pressure decrease at the end of drilling, but then you need also data on the permeability of the sand layer, which introduces some uncertainty.

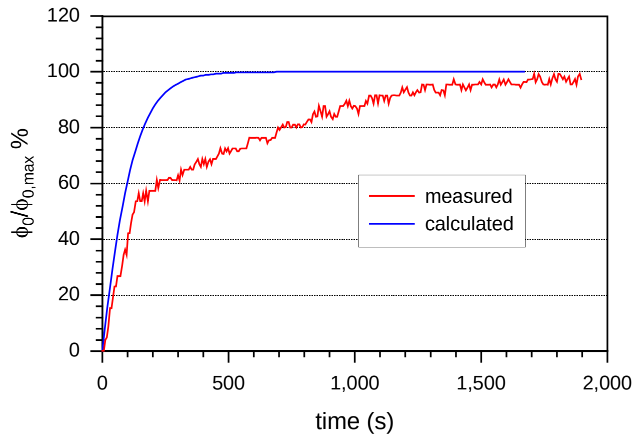

Figure 6: Measured and calculated pressure increas when drilling starts (GHT).

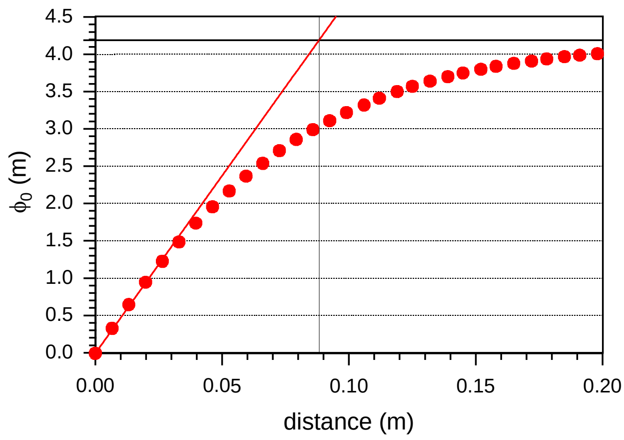

Figure 7: Estimated penetration depth from calculation.

2.3. CONCLUSIONS PORE PRESSURES

A calculation method is presented to show whether or not excess pore pressures will be present in front of a TBM when drilling in saturated sand. These excess pore pressures will decrease the stability of the tunnel face (Bezuijen et al. 2001, Aime et al. 2004, Kaalberg et al. 2014). The model presented also describes the pore pressure decrease when drilling stops and the increase in pore pressure when drilling starts. The interaction between soil and slurry or muck can be further improved but need experiments where muck and slurry penetration is performed at penetration velocities equal to the ones to be expected in front of a TBM.

3. PRESSURES AROUND A TBM SHIELD

Injection of the tail void grout with a higher pressure will generally lead to a reduction of the settlement trough due to boring. The wish to reduce the soil deformation has led to the use of higher grout pressures. See for example Figure 8. This figure shows the average grout pressure measured in the TBM for two tunnels, one constructed in 1999 and one in 2013. Both are tunnels with a diameter of around 10 m and the measurements are compared when the tunnels were at the same depth, as can be seen from the measured average grout pressures just before drilling starts, which is assumed to be roughly equal to the pore water pressure (Bezuijen et al., 2004). The duration of the high grout pressures is longer for the 2013 tunnel, because the drilling velocity for that tunnel is lower. Of importance is that the average grout pressure during drilling is significantly higher for the 2013 tunnel, while the pressures are quite comparable in the periods without drilling. It should be noted that the measured pressures are measured pressures are not measured in the tail void but for both tunnels in the TBM before the grout injection lines. This introduces an inaccuracy as can be seen in Figure 9, where grout pressures were measured as well in the tail of the TBM in the freshly injected grout in the tail void and before the grout injection lines (data from the Sophia Rail Tunnel, The Netherlands). It is shown that the flow resistance can result in a pressure difference of 0.75 bar during drilling and only a limited pressure difference during stand still. Although the pressure measurement in the TBM before the injection lines is thus an rather inaccurate measurement to obtain the grout pressures in the tail void and the grout properties may be different for the 1999 and 2013 tunnel, this cannot explain all differences between the measured grout pressures for these tunnels as shown in Figure 8 and they must have been significantly higher for the 2013 tunnel.

The high pressures resulted indeed in limited soil deformation for the 2013 tunnel. However, it should be noted that this also leads to an increase of the loading on the TBM shield. Both the tapering of the tunnel and the high grout pressures will cause a grout flow around the tail shield of the TBM. This is sometimes seen at the end of a TBM drive when the TBM is partly covered with grout, see Figure 10.

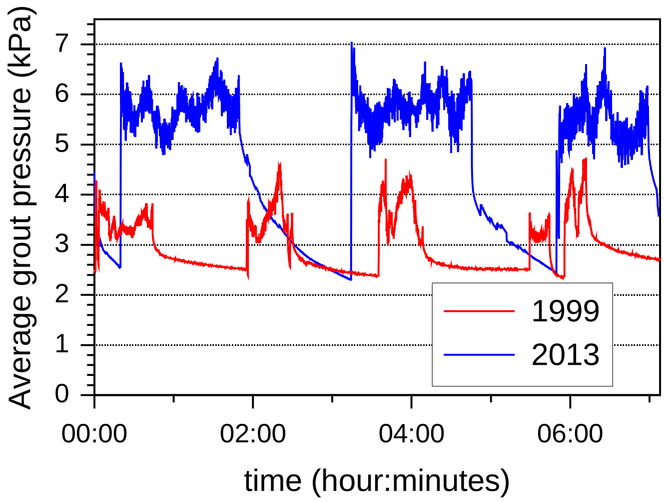

Figure 8: Comparison measured grout pressures for comparable tunnels drilled in 1999 and 2013, see further text.

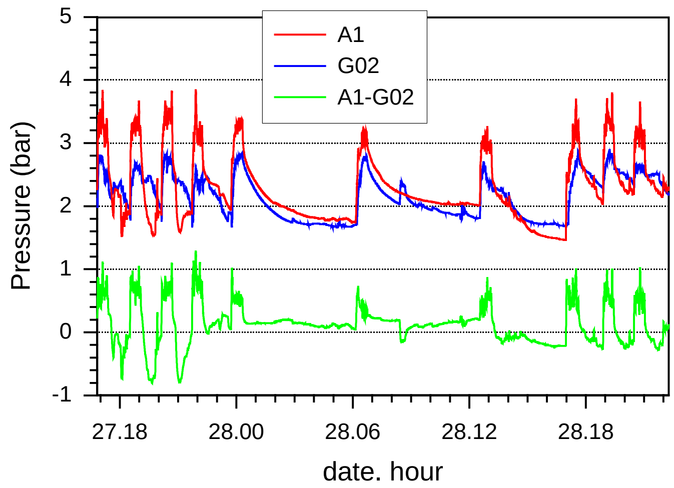

Figure 9: Sophia Rail tunnel, Groutpressures measured in TBM (A1), in tail void (G02) and difference (moving average over 11 points for A1 and difference to reduce fluctuation from plunger pump).

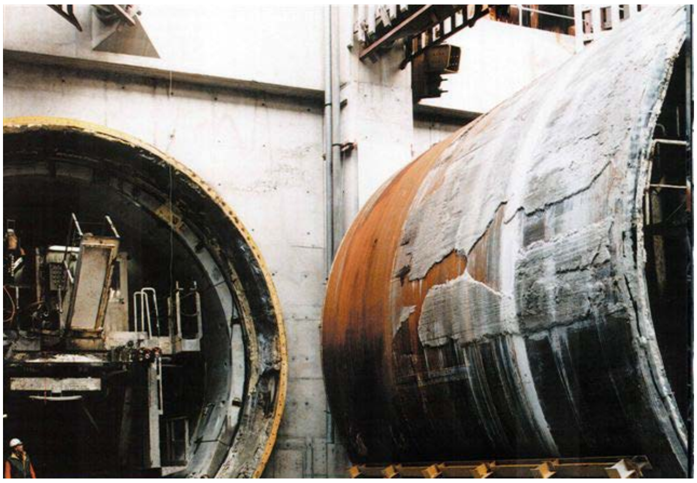

Figure 10: TBM 2nd Heinenoord tunnel after one drive. Grout on the shield is visible.

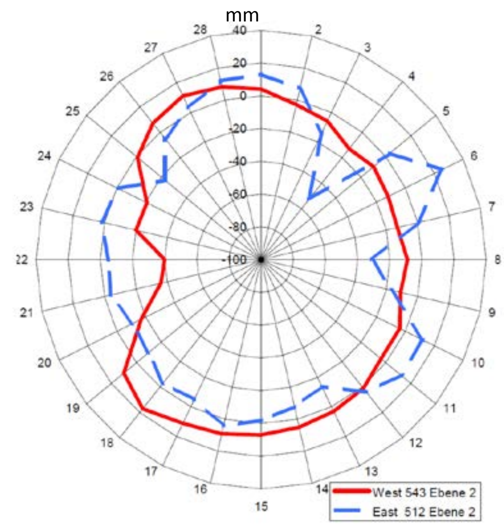

Figure 11: Deformations measured at the tail shield of a TBM. (Western-Scheldt Tunnel)

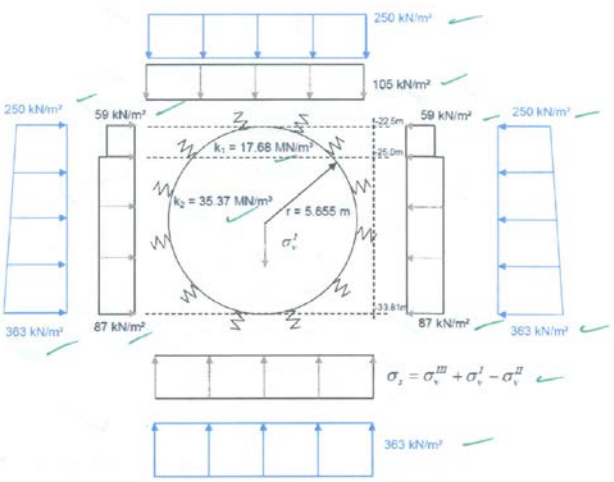

Figure 12: Boundary conditions as used for the design of the tail shield.

Remarkably this is not yet taken into account for the design of the TBM shield. At high pressures the tail of the TBM can deform (see Figure 11), making it difficult or impossible to install the lining.

Manufactures of TBM machines therefore perform 3-D finite element calculations to predict the maximum deformations. In these calculations the metal parts of the shield are modelled in 3-dimensions and the soil is modelled as springs, see Figure 12, taken from such a design report. The springs are 'pressure-springs'. They only work in pressure not in tension. These springs limit the deformations. When in reality the shield tail can deform 'freely' because it is in liquid, this will lead to larger deformations as was actually measured. What is also clear from Figure 12 that showed the cross-section with the highest pressures for the 2013 tunnel, is that the pressures taken into account are lower than the measured grout pressures. High grout pressures around the tunnel and some asymmetric loading on the tail due to curving of the tunnel leading to local soil contact (Festa, 2015) may have led to the higher measured deformations than predicted.

4. CONCLUSIONS

The following conclusions are possible from the measurements and theory presented in this paper:

- Excess pore pressures in front of a TBM can be expected when drilling in saturated sand. Close to the TBM this pore pressure will be equal to the pressure in the mixing chamber when the pore velocity of the grout water, calculated for a pressure equal to the pressure in the mixing chamber, is smaller than the drilling velocity. If the drilling velocity is lower, the excess pore pressure in front of the TBM can be calculated assuming that the slurry or muck enters the soil in front of the TBM with a velocity equal to the TBM velocity and this velocity has to be equal to the pore water velocity.
- The formulas developed allowed to describe the increase in pore pressure over time when drilling starts as well as the decrease when drilling stops.
- It is shown that a, the timespan to reach half of the final infiltration depth, as defined by Krause (1987) is not a material constant, but also depends on the radius of the tunnel and the permeability of the sand.
- Larger grouting pressures at the tail void will lead to smaller soil deformation, but higher loading on the tail shield of the TBM.

REFERENCES

[1] AIME R, ARISTAGHES P, AUTUORI P. and MINEC S., 2004. 15 m Diameter Tunneling under Netherlands Polders, Proc. Under-ground Space for Sustainable Urban Development (ITA Singapore), Elsevier pp. 1–8.

[2] Anagnostou G. & Kovári K., 1994. The face stability of Slurry-shield-driven Tunnels. Tunnelling and Underground Space Technology, Vol 9. No.2. pp 165-174.

[3] BAKKER K.J. & BEZUIJEN A., 2009. 10 years of bored tunnels in the Netherlands. Proceeding 6th Int. Symposium on Under-ground Construction in soft Ground, Shanghai, 2008, CRC Press/Balkema, Leiden.

[4] BEZUIJEN, A. & TALMON, A.M. 2009. Processes around a TBM. Proc. 6th Int. Symp. on Underground Construction in Soft Ground, Shanghai, 2008. CRC Press/Balkema, Leiden 3-13.

[5] BEZUIJEN A., TALMON A.M., KAALBERG F.J. and PLUGGE R., 2004. Field measurements of grout pressures during tunneling of the Sophia Rail tunnel. Soils and Foundations vol, 44, No 1, 41-50, February

[6] BEZUIJEN A., 2002. The influence of soil permeability on the properties of a foam mixture in a TBM. 3rd. Int. Symp. on Geotech. Aspects of Underground Construction in Soft Ground, IS-Toulouse

[7] BEZUIJEN A., PRUIKSMA J.P., MEERTEN H.H. van 2001. Pore pressures in front of tunnel, measurements, calculations and consequences for stability of tunnel face. Proc. Int. Symp. on Modern Tunneling Science and Techn. Kyoto.

[8] FESTA D. 2015, On the Interaction between a Tunnel Boring Machine and the Surrounding Soil. PhD_thesis, Delft University of Technology.

[9] KAALBERG F.J., DE NIJS R.E.P., and RUIGROK J.A.T. "TBM face stability & excess pore presssures in close proximity of piled bridge foundations controlled with 3D FEM". In: Geotechnical Aspects of Underground Construction in Soft Ground (2014), pp. 555–560.

[10] KRAUSE. T. (1987) Schildvortriebmit flüssigkeits- und erdgestützter Ortsbrust (PhD thesis) (in German).

[11] STEENEKEN, S.P. (2016) Excess pore pressures near a slurry tunnel boring machine: Modelling and measurements. Msc-thesis, Delft University of Technology, department Civil Engineering.

[12] TALMON A. M., MASTBERGEN D. R., and HUISMAN, M., 2013 "Invasion of pressurized clay suspensions into granular soil". In: Journal of Porous Media 16 pp. 351–365.